Laboratory activity 2: Digital position control of a DC servomotor

Riccardo Antonello* Francesco Ticozzi*

April 14, 2021

1 Activity goal

The goal of this laboratory activity is to design a digital position controller for the DC servomotor available in the laboratory. Two different design approaches are considered: in the *design by emulation*, the digital controller is obtained by discretization of a controller that is originally designed in the continuous–time domain; vice versa, in the *direct digital design* (or *discrete design*), the control design is performed directly in the discrete–time domain, using a discrete–time model of the plant to be controlled.

2 Sampled–data control system

A *sampled–data system* is a system where both continuous and discrete time signals coexist. A *sampled–data* or *digital control system* is a closed–loop control system where a continuous–time plant is controlled by a digital controller (see Fig 1).

The digital controller in Fig 1 operates on the *samples* $y[k]$, $k \in \mathbb{Z}$ of the analog plant output $y(t)$, $t \in \mathbb{R}$. The samples are collected at regularly spaced (under uniform sampling assumption) *sampling instants* $t_k = k\,T$; the positive constant T is the *sampling period*, and $f_s = 1/T$ is the *sampling frequency*. The sampling instants are provided by a *clock*.

The *analog–to–digital converter (ADC)* samples the continuous–time analog input $y(t)$ at the sampling instants t_k, and converts the sampled values $y(t_k)$ into binary numbers $y[k]$ with a finite number of bits. The ADC output $y[k]$ is a *digital signal*, i.e. it is a discrete–time, quantised–amplitude signal.

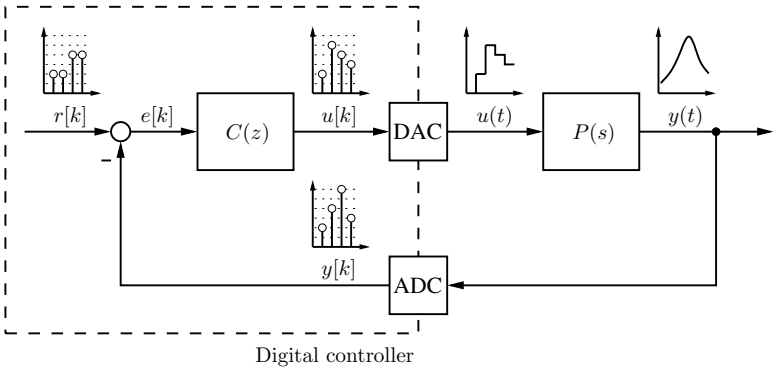

Figure 1: Sampled–data control system.

*Dept. of Information Engineering (DEI), University of Padova; email: {antonello, ticozzi}@dei.unipd.it

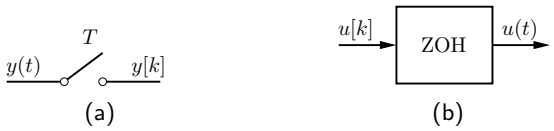

Figure 2: Idealised elements for sampled–data system analysis: (a) ideal sampler; (b) zero–order holder (ZOH).

The *digital–to–analog converter (DAC)* converts the digital signal $u[k]$ (digital controller output) into an analog signal $u(t)$. The conversion usually consists of holding the input value $u[k]$ over the whole *sampling interval* $[kT,\,(k+1)T)$ (analog reconstruction based on *zero–order holding*).

For the purpose of analysis and design, the ADC and DAC devices are replaced by their idealisations, namely the *ideal sampler* and the *(zero–order) holder* (ZOH):

- *Ideal sampler*: it periodically samples the continuous–time analog input $y(t)$ to yield the discrete time signal

$$y[k] \,=\, y(k\,T) \tag{1}$$

- *Zero–order holder*: it converts the discrete–time input signal $u[k]$ into a continuous–time signal $u(t)$ by holding it constant over the sampling intervals, i.e.

$$u(t) \,=\, u[k] \qquad \text{for} \qquad k\,T \,\leq\, t \,<\, (k+1)\,T \tag{2}$$

Note that the output $y[k]$ of the ideal sampler and the input $u[k]$ of the ZOH are not quantised in amplitude, i.e. they are not digital signals. Usually, a sampled–data system is regarded as an idealisation of a digital system, in which the amplitude quantisation of the digital signals is neglected. In a (single–rate) sample–data system, the ideal sampler and the ZOH are synchronised by the same clock: the ideal sampler instantaneously samples its input, and the ZOH output instantaneously jumps at the sampling instants.

3 Analysis of a sampled–data control system

There are fundamentally two alternative methods for analysing a sampled–data control system:

a) *analysis in continuous–time domain*: the series of the ideal sampler, the discrete–time controller and the ZOH (see Fig. 8) is described with an *approximate* continuous–time model.

b) *analysis in discrete–time domain*: the series of the ZOH, the continuous–time plant and the ideal sampler (see Fig. 3b) is described with an *approximate* discrete–time model.

Figure 3: Analysis of a sampled–data control system: (a) sampled–data controller; (b) sampled–data plant.

3.1 Analysis of a sampled–data control system in the continuous–time domain

The analysis in the continuous–time domain requires to define suitable continuous–time models of the ideal sampler and the ZOH, before deriving a continuos–time model of the sampled–data controller.

3.1.1 Continuous–time model of the ideal sampler

A continuous–time model model of the ideal sampler is the *impulsive sampler*, which is defined as a modulator with a train of Dirac impulses as the *carrier signal*, and the analog input to be sampled as the *modulating signal*. Let the carrier signal be defined as

$$\delta_T(t) \;=\; \sum_{k=-\infty}^{+\infty} \delta(t - kT) \tag{3}$$

Then the output of the impulsive sampler is (reminding the *revealing property* of the Dirac impulse, which states that $y(t)\,\delta(t-t_0) = y(t_0)\delta(t-t_0)$)

$$y^*(t) \;=\; y(t)\,\delta_T(t) \;=\; \sum_{k=-\infty}^{+\infty} y(kT)\,\delta(t - kT) \tag{4}$$

Note that both $y(t)$ and $y^*(t)$ are continuous–time signals. For the analysis of the sampled–data system, it is required to relate the Laplace ($\mathcal{L}$) and Fourier ($\mathcal{F}$) transforms

$$Y(s) \;=\; \mathcal{L}\left\{y(t)\right\}(s)\,, \qquad Y(j\omega) \;=\; \mathcal{F}\left\{y(t)\right\}(\omega) \tag{5}$$

of the impulsively sampled signal $y^*(t)$ with:

– the $\mathcal{L}$ and $\mathcal{F}$ transforms

$$Y(s) \;=\; \mathcal{L}\left\{y(t)\right\}(s)\,, \qquad Y(j\omega) \;=\; \mathcal{F}\left\{y(t)\right\}(\omega) \tag{6}$$

of the analog input $y(t)$.

– the Zeta ($\mathcal{Z}$) and Discrete–Time Fourier Transform (DTFT)

$$\bar{Y}(z) \;=\; \mathcal{Z}\left\{\bar{y}[k]\right\}(z)\,, \qquad \bar{Y}(e^{j\omega T}) \;=\; \mathcal{F}\left\{\bar{y}[k]\right\}(\omega) \tag{7}$$

of the discrete–time signal[1] $\bar{y}[k] = y(kT)$.

The following relationships can be established:

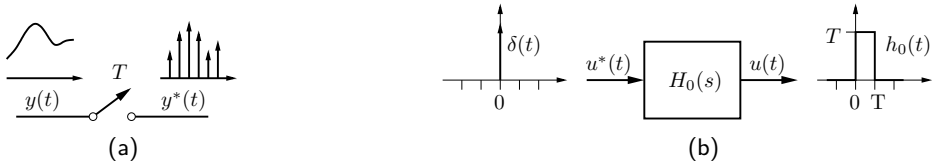

(a) (b)

Figure 4: Continuous–time models of the ideal sampler and the ZOH: (a) impulsive sampler; (b) continuous–time model of the ZOH.

[1] The definition of the new symbol $\bar{y}[k]$ in place of the original $y[k]$ is required in the following to avoid ambiguity in notation between the $\mathcal{L}$–transform of $y(t)$ and the $\mathcal{Z}$–transform of $y[k]$

a) relationship between $Y(s)$ and $Y^*(s)$.

The impulse train signal $\delta_T(t)$ is periodic, so that it can be decomposed into a Fourier series:

$$\delta_T(t) = \sum_{n=-\infty}^{+\infty} c_n \, e^{jn\omega_s t} \qquad \text{with} \qquad c_n = \frac{1}{T} \int_{-T/2}^{T/2} \delta_T(t) \, e^{-jn\omega_s t} \, dt \, = \, \frac{1}{T} \tag{8}$$

where $\omega_s = 2\pi f_s$ is the sampling frequency in $[\mathrm{rad/s}]$ units. Then, from (4) it follows that

$$Y^*(s) \, = \, \mathcal{L}\left\{y^*(t)\right\}(s) \, = \, \frac{1}{T} \sum_{n=-\infty}^{+\infty} \mathcal{L}\left\{y(t) e^{jn\omega_s t}\right\}(s) \, = \, \frac{1}{T} \sum_{n=-\infty}^{+\infty} Y(s - jn\omega_s) \tag{9}$$

b) relationship between $Y^*(s)$ and $\bar{Y}(z)$.

By applying the definition of the Laplace transform to the impulsively sampled signal (4), it follows that

$$\begin{aligned} Y^*(s) = \mathcal{L}\left\{y^*(t)\right\}(s) = \int_0^{+\infty} y^*(t) \, e^{-st} \, dt = \int_0^{+\infty} \sum_{n=-\infty}^{+\infty} y(t) \, \delta(t - nT) \, e^{-st} \, dt \\ \cdots \quad = \sum_{n=0}^{+\infty} y(nT) e^{-snT} = \sum_{n=0}^{+\infty} \bar{y}[n] \left(e^{sT}\right)^{-n} = \bar{Y}(z)\Big|_{z=e^{sT}} \end{aligned} \tag{10}$$

namely the $\mathcal{L}$–transform of $y^*(t)$ coincides with the $\mathcal{Z}$–transform of $\bar{y}[k]$ evaluated at $z = e^{sT}$. In particular, the map $z = e^{sT}$ establishes a connection between the s–plane of the Laplace transform and the z–plane of the $\mathcal{Z}$–transform.

c) relationship between $Y^*(j\omega)$, $\bar{Y}\left(e^{j\omega T}\right)$ and $Y(j\omega)$.

By setting $s = j\omega$ in (9), and by using also (10), it follows that:

$$Y^*(j\omega) \, = \, \bar{Y}\left(e^{j\omega T}\right) \, = \, \frac{1}{T} \sum_{n=-\infty}^{+\infty} Y\left(\, j(\omega - n\omega_s) \,\right) \tag{11}$$

In particular, $Y^*(j\omega)$ is obtained as the sum of infinitely many replicas of $Y(j\omega)$, that are frequency shifted by multiplies of ω_s. The relationship (11) admits the graphical representation reported in Fig. 5. Assume that the continuous–time signal $y(t)$ has the band–limited spectrum $Y(j\omega)$ shown in Fig. 5a, whose support is the interval $[-\omega_B, \omega_B]$. For graphical convenience, assume that $Y(j\omega) \in \mathbb{R}$ (in general, the spectrum is a complex value quantity, i.e. $Y(j\omega) \in \mathbb{C}$). Let $\omega_N = \omega_s/2$ denotes the *Nyquist frequency*. If the signal band ω_B is smaller than the Nyquist frequency, i.e. $\omega_B < \omega_N$, then the spectrum of the sampled signal is as shown in Fig. 5b, in which the frequency–shifted replicas of $Y(j\omega)$ do not overlap. On the other hand, if the signal band ω_B is larger than the Nyquist frequency, i.e. $\omega_B > \omega_N$, then adjacent frequency–shifted replicas of $Y(j\omega)$ do overlap, giving rise to the so called *aliasing phenomenon*. Reconstruction of the original continuous–time signal from the sampled one is possible only when the aliasing phenomenon does not occur, as stated by the *Shannon's sampling theorem*.

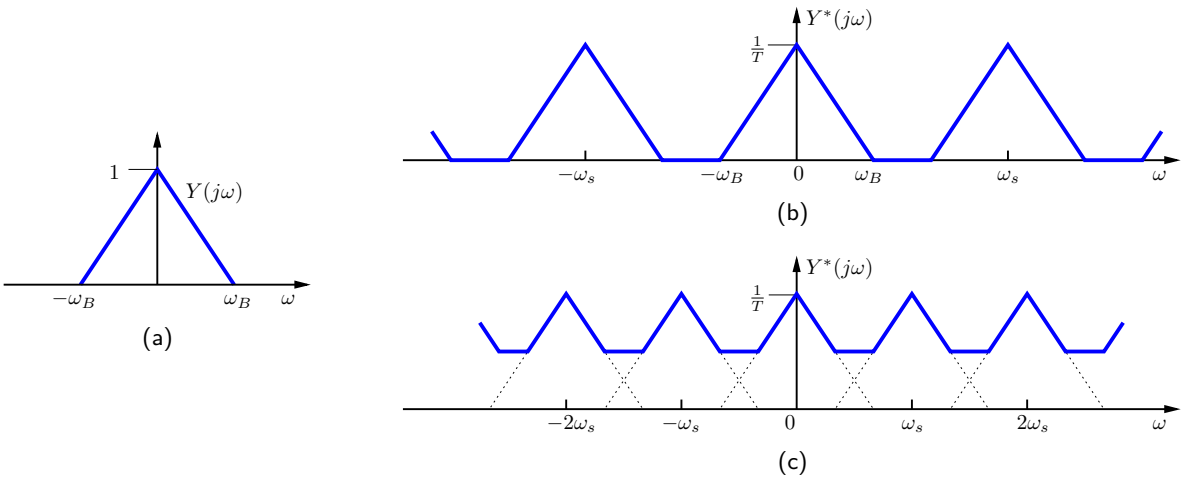

Figure 5: Graphical interpretation of the spectrum of a sampled signal: (a) spectrum of the original band–limited signal; (b) spectrum of the sampled signal when $\omega_B < \omega_s/2$; (c) spectrum of the sampled signal when $\omega_B > \omega_s/2$ (*aliasing phenomenon*).

Theorem (*Shannon's sampling theorem*)**.**
Let $y(t)$ be a continuos-time signal with with a band-limited spectrum, i.e. $|Y(j\omega)| = 0$ for $|\omega| > \omega_B$. If

$$\omega_B < \omega_N \tag{12}$$

with $\omega_N = \omega_s/2 = \pi/T$ denoting the *Nyquist frequency*, the the signal $y(t)$ can be exactly reconstructed from the (impulsively) sampled signal $y^*(t)$. The reconstruction can be performed by filtering $y^*(t)$ with a "brick–wall" low-pass filter (also known as *sinc–filter*) of the type:

$$H(j\omega) = \begin{cases} T & -\omega_N \leq \omega \leq \omega \\ 0 & \text{otherwise} \end{cases} \tag{13}$$

□

The reconstruction process with a "brick–wall" low–pass filter is graphically depicted in Fig. 6.

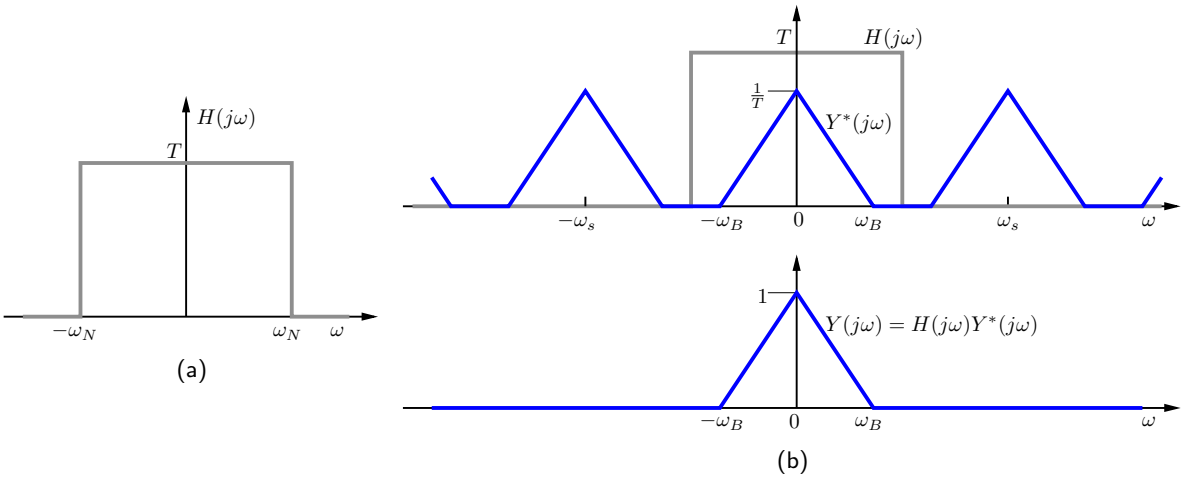

Figure 6: Reconstruction of a continuous–time signal from its sampled version (satisfying the conditions of the Shannon's sampling theorem): (a) reconstruction filter; (b) reconstruction process.

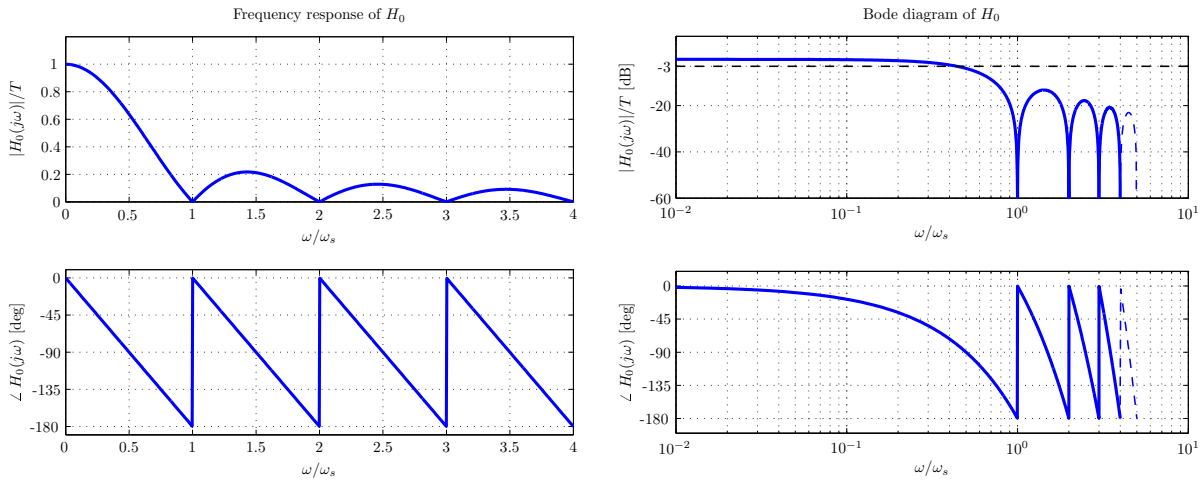

(a) (b)

Figure 7: Frequency response of the filter $H_0(s)$: (a) linear scale plot; (b) logarithmic scale plot (Bode plot).

3.1.2 Continuous–time model of the zero–order holder

A continuous–time model of the ZOH can be obtained by replacing the discrete-time input $u[k]$ with its impulsively sampled version $u^*(t)$. After replacing $u[k]$ with $u^*(t)$, the ZOH can be modelled as a continuos–time filter with impulse response $h_0(t)$ given by (see also Fig. 4b):

$$h_0(t) \;=\; \delta_{-1}(t) \;-\; \delta_{-1}(t-T) \tag{14}$$

where $\delta_{-1}(t)$ denotes the unit step, applied at the origin. The transfer function is

$$H_0(s) \;=\; \mathcal{L}\{h_0(t)\}(s) \;=\; \frac{1}{s} \;-\; \frac{e^{-s\,T}}{s} \;=\; \frac{1-e^{-s\,T}}{s} \tag{15}$$

The frequency response is obtained by substituting $s = j\omega$ in the expression of the transfer function: it holds that

$$H_0(j\omega) \;=\; \frac{1-e^{-j\omega T}}{j\omega} \;=\; e^{-j\omega T/2}\,\frac{e^{j\omega T/2}-e^{-j\omega T/2}}{j\omega} \;=\; T\,e^{-j\omega T/2}\,\frac{\sin\left(\omega T/2\right)}{\omega T/2} \tag{16}$$

The frequency response is shown in Fig. 7, both in linear and logarithmic (Bode plot) scales.

3.1.3 Continuous–time model of the sampled–data controller

Consider the sampled–data controller shown in Fig. 8a, consisting of the series of the the ideal sampler, the discrete–time controller and the ZOH. A continuous–time model is obtained by first replacing the discrete–time output $\bar{u}[k]$ with its impulsively sampled version $u^*(t)$, and the ZOH with with the filter $H_0(s)$ defined in Sec. 3.1.2. Then, by using (10), it follows that

$$U(z) \;=\; C(z)\,E(z) \qquad \underset{U^*(s)=\bar{U}(e^{sT})}{\Longrightarrow} \qquad U^*(s) \;=\; C\left(e^{sT}\right)\,E^*(s) \tag{17}$$

Define $C^*(s) \;=\; C\left(e^{sT}\right)$; then, the continuous–time model of the sampled–data controller is as shown in Fig. 8b. The transfer function from the continuous–time input $E(t)$ to the continuous–

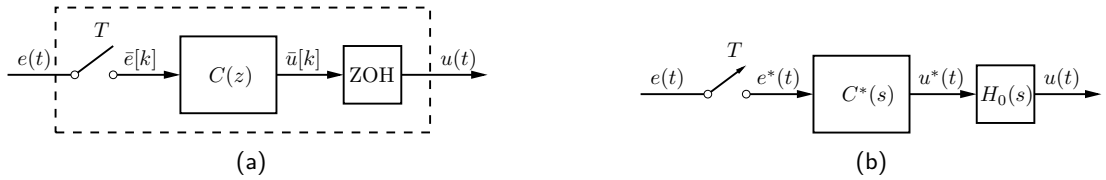

Figure 8: Continuous–time model of a sampled–data controller: (a) original controller; (b) continuous–time model.

time output $U(t)$ is

$$U(s) \;=\; H_0(s)\, C^*(s)\, E^*(s) \qquad \text{with} \qquad E^*(s) \;=\; \frac{1}{T} \sum_{n=-\infty}^{+\infty} E(s - jn\omega_s) \tag{18}$$

By setting $s = j\omega$ in (18) if follows that

$$U(j\omega) = H_0(j\omega) C^*(j\omega) E^*(j\omega) \qquad \text{with} \qquad E^*(j\omega) = \frac{1}{T} \sum_{n=-\infty}^{+\infty} E(j(\omega - n\omega_s)) \tag{19}$$

If the input e is band–limited, with bandwidth $\omega_B < \omega_N$, then the following approximation can be introduced:

$$E^*(j\omega) H_0(j\omega) \approx \frac{1}{T} E(j\omega) H_0(j\omega) \qquad \forall\, \omega \in [0, +\infty) \tag{20}$$

The approximation is valid because $H_0(s)$ is a low–pass filter with cut-off frequency smaller than ω_N, and therefore all the frequency–shifted replicas of $E(j\omega)$ beyond the Nyquist frequency are well attenuated. By using the approximation (20) in (19) it follows that

$$U(j\omega) \approx \frac{1}{T} H_0(j\omega) C^*(j\omega) E(j\omega) \qquad \text{for} \qquad \omega \in [0, +\infty) \tag{21}$$

Moreover, by noting that

$$H_0(j\omega) \approx T\, e^{-j\omega T/2} \qquad \text{for} \qquad |\omega| \leq \omega_N \tag{22}$$

the expression (21) can be further reduced to

$$U(j\omega) \approx e^{-j\omega T/2}\, C^*(j\omega)\, E(j\omega) \qquad \text{for} \qquad \omega \in [0, \omega_N) \tag{23}$$

Therefore, under the hypothesis of a band–limited input signal e, with bandwidth $\omega_B < \omega_N$, the frequency response of the continuous–time model is

$$\frac{U(j\omega)}{E(j\omega)} \approx \frac{1}{T}\, H_0(j\omega)\, C^*(j\omega) \qquad \text{for} \qquad \omega \in [0, +\infty) \tag{24}$$

or

$$\frac{U(j\omega)}{E(j\omega)} \approx e^{-j\omega T/2}\, C^*(j\omega) \qquad \text{for} \qquad \omega \in [0, \omega_N) \tag{25}$$

where $C^*(j\omega) = C(e^{j\omega T})$. By using the the substitution $s = j\omega$ in (24), the following transfer function for the continuous–time model can be immediately obtained

$$\frac{U(s)}{E(s)} \;\approx\; \frac{1}{T}\, H_0(s)\, C^*(s) \qquad \text{where} \qquad C^*(s) = C(e^{sT}) \tag{26}$$

3.2 Analysis of a sampled–data control system in the discrete–time domain

The analysis in the discrete–time domain requires to define a suitable discrete–time model of the series connection of the ZOH, the plant and the ideal sampler (sampled–data plant, see Fig. 3b). Let $\Sigma = (\boldsymbol{A}, \boldsymbol{B}, \boldsymbol{C}, D)$ be a state–space model of the plant [2]. By using the *Lagrange's formula*

$$\boldsymbol{x}(t) \;=\; \boldsymbol{e}^{\boldsymbol{A}(t-t_0)}\,\boldsymbol{x}(t_0) \;+\; \int_{t_0}^{t} \boldsymbol{e}^{\boldsymbol{A}(t-\tau)}\,\boldsymbol{B}\,u(\tau)\,d\tau \tag{27}$$

with $t_0 = k\,T$ and $t = (k+1)T$, it follows that

$$\boldsymbol{x}((k+1)T) \;=\; \boldsymbol{e}^{\boldsymbol{A}T}\,\boldsymbol{x}(kT) \;+\; \int_{kT}^{(k+1)T} \boldsymbol{e}^{\boldsymbol{A}[(k+1)T-\tau]}\,\boldsymbol{B}\,u(\tau)\,d\tau \tag{28}$$

Because of the presence of the ZOH, the input $u(\tau)$ is constant and equal to $u[k]$ when $\tau \in [kT, (k+1)T)$. Therefore

$$\begin{aligned} \boldsymbol{x}((k+1)T) \;&=\; \boldsymbol{e}^{\boldsymbol{A}T}\,\boldsymbol{x}(kT) \;+\; \left[\int_{kT}^{(k+1)T} \boldsymbol{e}^{\boldsymbol{A}[(k+1)T-\tau]}\,\boldsymbol{B}\,d\tau\right] u(kT) \\ &=\; \underbrace{\boldsymbol{e}^{\boldsymbol{A}T}}_{\triangleq\,\boldsymbol{\Phi}}\,\boldsymbol{x}(kT) + \underbrace{\left[\int_0^{T} \boldsymbol{e}^{\boldsymbol{A}\eta}\boldsymbol{B}\,d\eta\right]}_{\triangleq\,\boldsymbol{\Gamma}} u(kT) \end{aligned} \tag{29}$$

which yields the discrete–time plant model

$$\begin{cases} \boldsymbol{x}[k+1] \;=\; \boldsymbol{\Phi}\,\boldsymbol{x}[k] \;+\; \boldsymbol{\Gamma}\,u[k] \\ \qquad y[k] \;=\; \boldsymbol{C}\,\boldsymbol{x}[k] \;+\; D\,u[k] \end{cases} \tag{30}$$

whose input–output transfer function from $u[k]$ to $y[k]$ is equal to

$$P(z) \;=\; \boldsymbol{C}\,(z\,\boldsymbol{I} - \boldsymbol{\Phi})^{-1}\,\boldsymbol{\Gamma} \;+\; D \tag{31}$$

There is a strict relationship between the eigenvalues of the original continuous–time plant model and its discretised version, which is summarised in the following fact.

Fact (*Relationship between continuous and discrete time plant eigenvalues*)**.**
The eigenvalues $s_i \in \mathbb{C}$, $i = 1, \ldots, n$ of $\boldsymbol{A}$ are related to the eigenvalues $z_i \in \mathbb{C}$ of $\boldsymbol{\Phi} = \boldsymbol{e}^{\boldsymbol{A}T}$ by the relation:

$$z_i \;=\; e^{s_i T} \qquad i = 1, \ldots, n \tag{32}$$

In particular:

1. the imaginary axis $s = j\omega$ is mapped into the unit circle $|z| = 1$
2. the point $s = 0$ is mapped into the point $z = 1$
3. the LHP in the s-plane is mapped into the region within the unit circle in the z-plane

□

[2] A SISO plant is considered in the following: however, the analysis reported in this section can be immediately extended, without any particular change, to the MIMO case.

The proof of (32) is immediate, since if $\lambda \in \mathbb{C}$ is an eigenvalue of the matrix $\boldsymbol{A}$ with associated eigenvector $\boldsymbol{v}$, then $e^{\lambda t}$ is an eigenvalue of the matrix exponential $\boldsymbol{e}^{\boldsymbol{A}t}$ with the same associated eigenvector $\boldsymbol{v}$. By using the transformation $z = e^{sT}$, it is possible to determine how the specific regions of the s–plane are mapped into the z–plane. The interesting regions are

1. region of eigenvalues associated with system modes having a decaying ratio faster than the exponential $e^{\sigma_0 t}$, namely the region

$$S_\sigma \;=\; \{s = \sigma + j\omega \in \mathbb{C} \,:\, \sigma < \sigma_0,\; \omega \in \mathbb{R}\} \tag{33}$$

   The region S_σ and its corresponding region in the z–plane are shown in Fig. 10a.

2. region of eigenvalues having a damping ratio greater than δ_0, namely

$$S_\delta \;=\; \{s = -\delta\,\omega_n \pm j\omega_n\sqrt{1-\delta^2} \in \mathbb{C} \;\;:\;\; 0 \,\leq\, \delta \,\leq\, \delta_0 \,<1, \quad \omega_n > 0\} \tag{34}$$

   The region S_δ and its corresponding region in the z–plane are shown in Fig. 10b.

3. region of eigenvalues having a natural frequency smaller than ω_{n0}, namely

$$S_\omega \;=\; \{s = -\delta\,\omega_n \pm j\omega_n\sqrt{1-\delta^2} \in \mathbb{C} \;\;:\;\; 0 \leq \delta \leq 1, \quad 0 \leq \omega_n \leq \omega_{n0}\} \tag{35}$$

   The region S_δ and its corresponding region in the z–plane are shown in Fig. 10c.

It is worth to notice that the map $z = e^{sT}$ from the s–plane to the z–plane is not bijective: in fact, given $s_0 \in \mathbb{C}$, the points $s = s_0 + jk\frac{2\pi}{T}$ are mapped into the same point in the z-plane. This is equivalent to say that stripe regions of height $2\pi/T$ in the s–plane are mapped into the interior or the exterior of the unit disc in the z–plane, depending on whether the stripe extends in the left or right half part of the s–plane. For stripes extending in the left–half complex plane, the correspondence with the interior of the unit disc in the z–plane is illustrated in Fig. 9. Note that the map $z = e^{sT}$ becomes bijective when $s \in \mathbb{C}$ is restricted to lie within a single horizontal stripe of height $2\pi/T$ in the s–plane.

Note: according to the discretization procedure summarised in (27)–(30) (known as *exact* discretization method), a state–space model is required to obtain the discrete–time transfer function (31). An

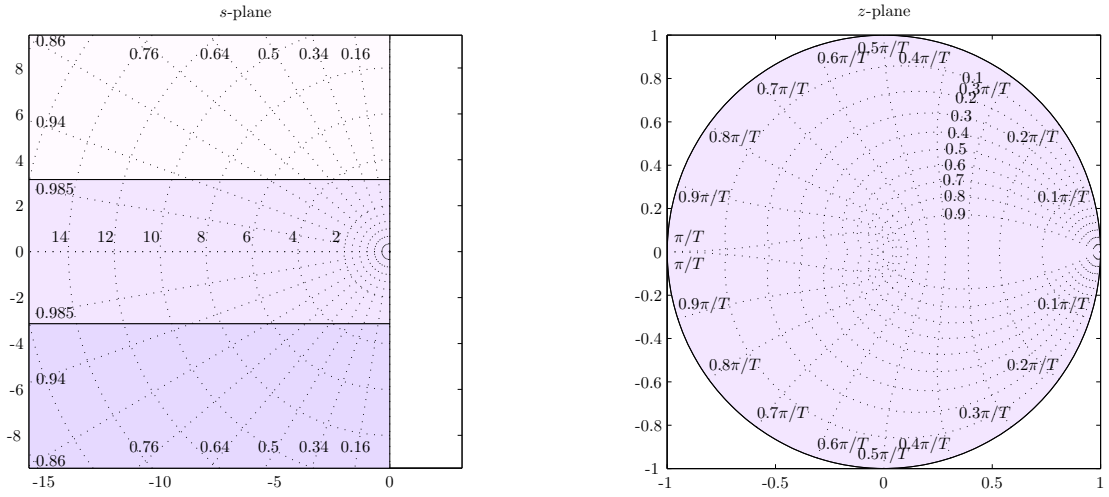

Figure 9: Non–bijectivity of the transformation $z = e^{sT}$.

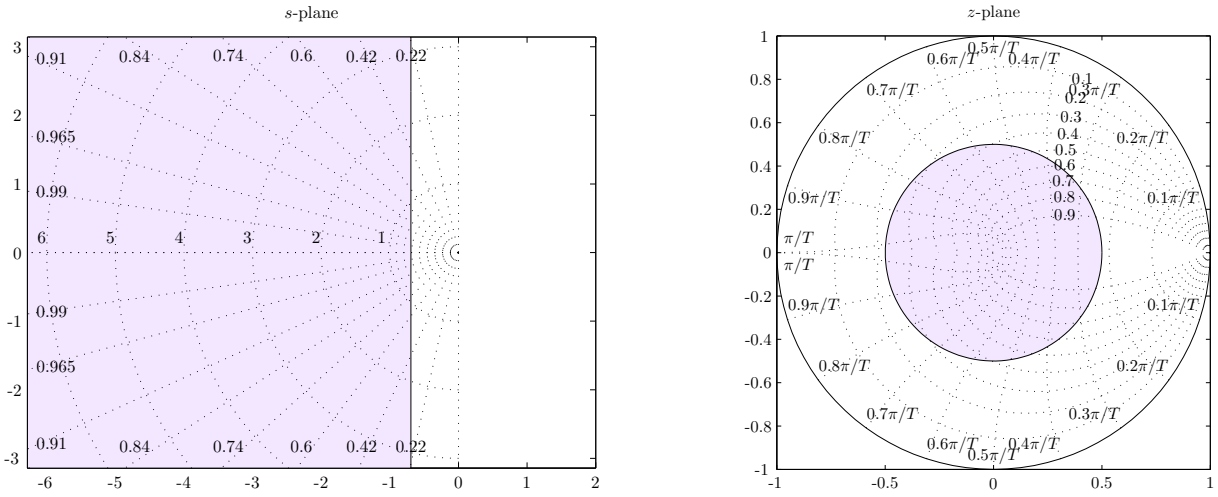

(a) Eigenvalues with system modes decaying faster than $e^{\sigma_0 t}$.

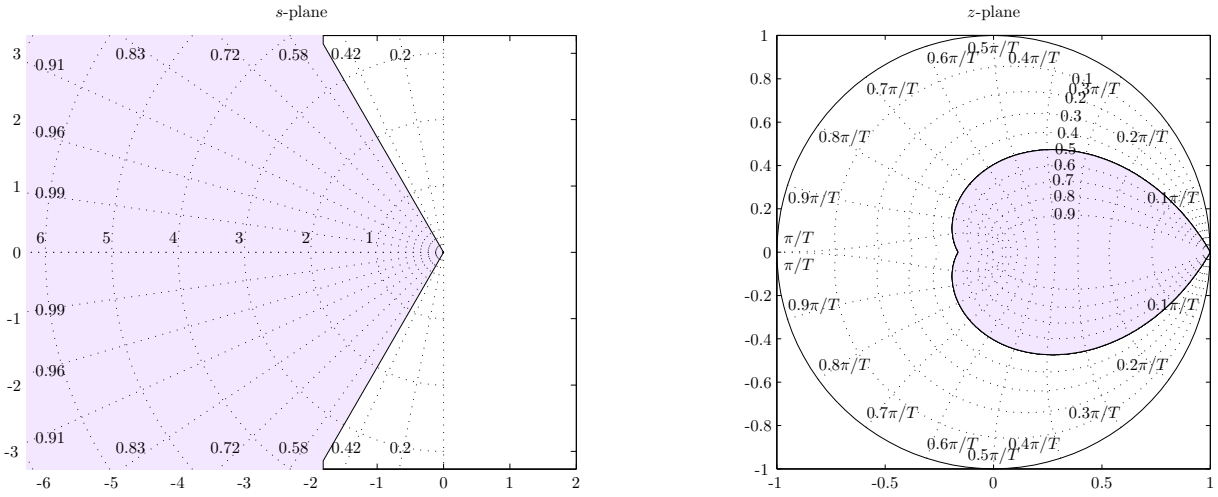

(b) Eigenvalues with damping ratio greater than δ_0.

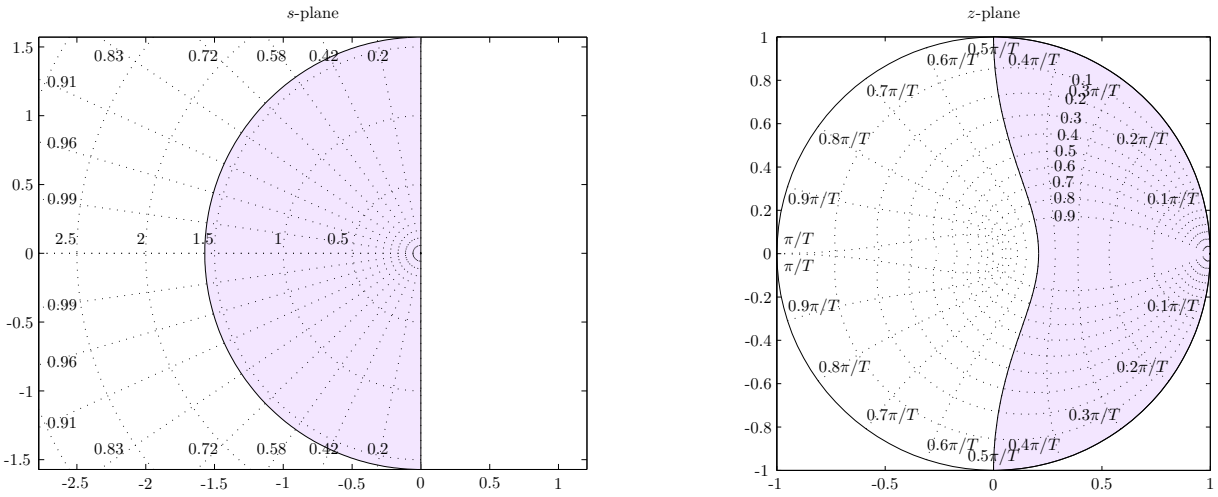

(c) Eigenvalues with natural frequency smaller than ω_{n0}.

Figure 10: Correspondences between the s and z planes, according to the transformation $z = e^{sT}$.

alternative method to obtain (31) without resorting to any state–space model is as follows. Consider to apply a unit discrete–time impulse $u[k] = \delta[k]$ to the input of a sampled–data plant such as that shown in Fig. 3b. The output $u(t)$ of the ZOH is

$$u(t) \;=\; \delta_{-1}(t) \;-\; \delta_{-1}(t-T) \tag{36}$$

whose $\mathcal{L}$–transform is equal to

$$U(s) \;=\; \mathcal{L}\left\{u(t)\right\}(s) \;=\; \frac{1-e^{-sT}}{s} \tag{37}$$

The $\mathcal{L}$–transform of the plant output is

$$Y(s) \;=\; P(s)\,U(s) \;=\; P(s)\,\frac{1-e^{-sT}}{s} \tag{38}$$

The time–domain response can be obtained by inverse $\mathcal{L}$–transformation, i.e.

$$y(t) \;=\; \mathcal{L}^{-1}\left\{P(s)\,U(s)\right\}(t) \;=\; \mathcal{L}^{-1}\left\{\frac{P(s)}{s}\right\}(t) \;-\; \mathcal{L}^{-1}\left\{\frac{P(s)}{s}\right\}(t-T) \tag{39}$$

The sampled version of (39), namely $y[k] = y(kT)$, is the discrete–time impulse response of the sampled–data plant: therefore, the $\mathcal{Z}$–transform of $y[k]$ is the discrete–time transfer function of the sampled–data plant. It holds that:

$$\begin{aligned} P(z) \;&=\; \mathcal{Z}\left\{y[k]\right\}(z) \\ &=\; \mathcal{Z}\left\{\mathcal{L}^{-1}\left\{\frac{P(s)}{s}\right\}(kT) \;-\; \mathcal{L}^{-1}\left\{\frac{P(s)}{s}\right\}(kT-T)\right\}(z) \\ &=\; \left(1-z^{-1}\right)\mathcal{Z}\left\{\mathcal{L}^{-1}\left\{\frac{P(s)}{s}\right\}(kT)\right\}(z) \end{aligned} \tag{40}$$

Introduce the definition

$$\mathcal{Z}\left\{\frac{P(s)}{s}\right\}(z) \;\triangleq\; \mathcal{Z}\left\{\mathcal{L}^{-1}\left\{\frac{P(s)}{s}\right\}(kT)\right\}(z) \tag{41}$$

which represents the $\mathcal{Z}$–transform of the sampled version of the unit step response of the continuous–time plant. Then, the transfer function (40) can be rewritten as follows

$$P(z) \;=\; \left(1-z^{-1}\right)\,\mathcal{Z}\left\{\frac{P(s)}{s}\right\}(z) \tag{42}$$

which is another way (alternative to (31)) of expressing the discrete–time transfer function of the sampled–data plant depicted in Fig. 3b. Differently from (31), note that no plant state–space model is required to evaluate (42): indeed, the only information required in this case is the plant transfer function $P(s)$ or, alternatively, the plant unit step response $\mathcal{L}^{-1}\{P(s)/s\}(t)$.

4 Design of a sampled–data control system

There are fundamentally two alternative methods for designing a sampled–data control system:

a) *design in continuous–time domain* (*design by emulation*): the control design is performed in the continuous–time domain, using either classical design methods (e.g. Bode's method, root locus method, etc.) or modern design methods (e.g. state–space methods).

   Then, a discrete–time controller approximating the response of the original continuous-time controller is obtained by applying a *discretization procedure*.

b) *design in discrete–time domain* (*direct digital design*, or *discrete design*): the control design is performed directly in the discrete–time domain, after obtaining a discrete–time model of the plant to be controlled with the methods explained in Sec. 3.2 (*exact* discretization of the continuous–time plant model).

4.1 Design by emulation

Say $C_0(s)$ the transfer function of the controller designed in continuous–time domain using either classical or modern design methods. The *discretization problem* consists of finding a discrete-time controller $C(z)$ such that the input–output transfer function of the sampled–data controller shown in Fig. 8, say $D(s)$, approximates (in some sense) the transfer function $C_0(s)$.

If the input $e(t)$ satisfies the hypothesis of the sampling theorem, then, according to (26), the transfer function of the sampled–data controller is

$$D(s) \,=\, \frac{1}{T}\, H_0(s)\, C^*(s) \,=\, \frac{1}{T}\, H_0(s)\, C(e^{sT}) \tag{43}$$

In the frequency range $[0,\, \omega_N)$ it holds that:

$$D(s) \approx e^{-sT/2}\, C(e^{sT})$$

In order to have $D(s) \approx C_0(s)$, it is necessary that:

$$e^{-sT/2}\, C(e^{sT}) \,\approx\, C_0(s) \qquad \Rightarrow \qquad C(e^{sT}) \,\approx\, e^{sT/2}\, C_0(s) \tag{44}$$

Therefore, a possible choice for the discretised controller $C(z)$ is obtained from (44) by using the inverse of the transformation of $z = e^{sT}$, namely $s = (1/T)\, \log\, z$. It follows that

$$C(z) \,=\, e^{sT/2}\, C_0(s)\,\Big|_{s=\frac{1}{T}\log z} \tag{45}$$

The problem with the transfer function (45) is that it is not rational, even if $C_0(s)$ is rational. Therefore, in order to overcome this issue, alternative discretization methods that produce rational transfer functions will be introduced in the following.

Let $C_0(s)$ be the transfer function of the controller designed in the continuous–time domain, and $\Sigma_C = (\boldsymbol{A},\, \boldsymbol{B},\, \boldsymbol{C},\, D)$ a possible state–space realisation. Then, the equation of the state evolution

$$\dot{\boldsymbol{x}}(t) \,=\, \boldsymbol{f}\,(\boldsymbol{x}(t),\, e(t)) \,=\, \boldsymbol{A}\,\boldsymbol{x}(t) \,+\, \boldsymbol{B}\, e(t) \tag{46}$$

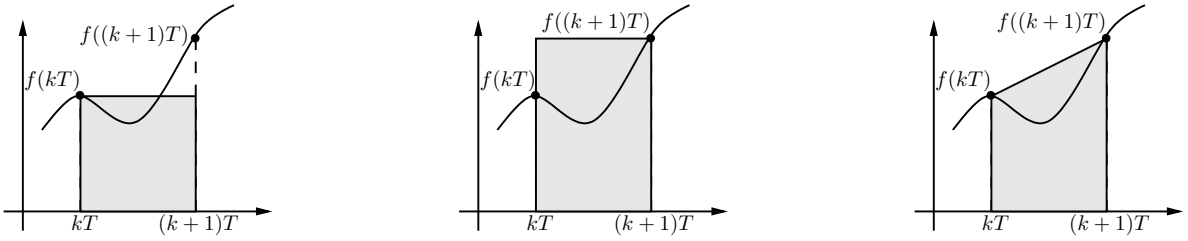

(a) $\alpha = 0$ (b) $\alpha = 1$ (c) $\alpha = 1/2$

Figure 11: Discretization methods: (a) forward Euler method; (b) backward Euler method; (c) trapezoidal (Tustin's) method.

can be integrated to yield

$$\boldsymbol{x}((k+1)T) \,=\, \boldsymbol{x}(kT) \,+\, \int_{kT}^{(k+1)T} \boldsymbol{f}\left(\boldsymbol{x}(\tau),\, e(\tau)\right)\, d\tau \tag{47}$$

The following approximation can be introduced

$$\begin{aligned} \int_{kT}^{(k+1)T} \boldsymbol{f}(\boldsymbol{x}(\tau),\, e(\tau))\, d\tau \;\approx\; T\,[\,(1-\alpha)\,\boldsymbol{f}(\boldsymbol{x}(kT),\, e(kT)) \,+\, \cdots \\ \cdots \,+\, \alpha\,\boldsymbol{f}(\boldsymbol{x}((k+1)T),\, e((k+1)T))\,] \end{aligned} \tag{48}$$

where $\alpha \,\in\, [0,1]$. The graphical interpretation of the approximation (48) is shown in Fig. 11, under the assumption of a scalar function $\boldsymbol{f}$. The approximation formula introduced above yields:

$$\boldsymbol{x}[k+1] - \boldsymbol{x}[k] \,=\, \boldsymbol{A}\,(\,(1-\alpha)\,\boldsymbol{x}[k] \,+\, \alpha\,\boldsymbol{x}[k+1]\,)\,T \,+\, \boldsymbol{B}\,(\,(1-\alpha)\,e[k] \,+\, \alpha\,e[k+1]\,)\,T \tag{49}$$

By applying the $\mathcal{Z}$-transform at both sides of the previous expression it follows that:

$$\left(\frac{1}{T}\,\frac{z-1}{\alpha z+1-\alpha}\boldsymbol{I} \,-\, \boldsymbol{A}\right)\boldsymbol{X}(z) \,=\, \boldsymbol{B}\,E(z) \tag{50}$$

By using the output equation $u[k] = \boldsymbol{C}\boldsymbol{x}[k] + De[k]$, it finally follows that:

$$C(z) \,=\, \frac{U(z)}{E(z)} \,=\, \boldsymbol{C}\left(\frac{1}{T}\,\frac{z-1}{\alpha z+1-\alpha}\boldsymbol{I} \,-\, \boldsymbol{A}\right)^{-1}\boldsymbol{B} + D \,=\, C_0(s)\,\Big|_{s\,=\,\frac{1}{T}\frac{z-1}{\alpha z+1-\alpha}} \tag{51}$$

where the last identity holds because $C_0(s) = \boldsymbol{C}\,(s\boldsymbol{I} - \boldsymbol{A})^{-1} + D$. The conclusion is that a discrete–time approximation of the continuous–time controller with transfer function $C_0(s)$ is obtained by performing the substitution:

$$C_0(s) \quad \xrightarrow[\text{Discretization}]{s\,=\,\frac{1}{T}\frac{z-1}{\alpha z+1-\alpha}} \quad C(z) \tag{52}$$

Note that with the variable substitution reported in (52), the discretization of a rational continuous–time transfer–function $C_0(s)$ is again a rational transfer function. Depending on the choice of α, several discretization methods can be defined, as reported in Tab. 1. It is worth to notice that all the variable substitutions defined in Tab. 1 are indeed rational approximations of the transformation $z = e^{sT}$, obtained by using the *Padé approximation* method. Depending on the variable substitution (and hence the discretization method) used, the left–half s–plane is mapped into different regions

Discretization method		Variable substitution
Forward Euler	$\alpha = 0$	$s = \dfrac{z-1}{T}$
Backward Euler	$\alpha = 1$	$s = \dfrac{z-1}{T\,z}$
Trapezoidal/Tustin	$\alpha = 1/2$	$s = \dfrac{2}{T}\dfrac{z-1}{z+1}$

Table 1: Discretization methods.

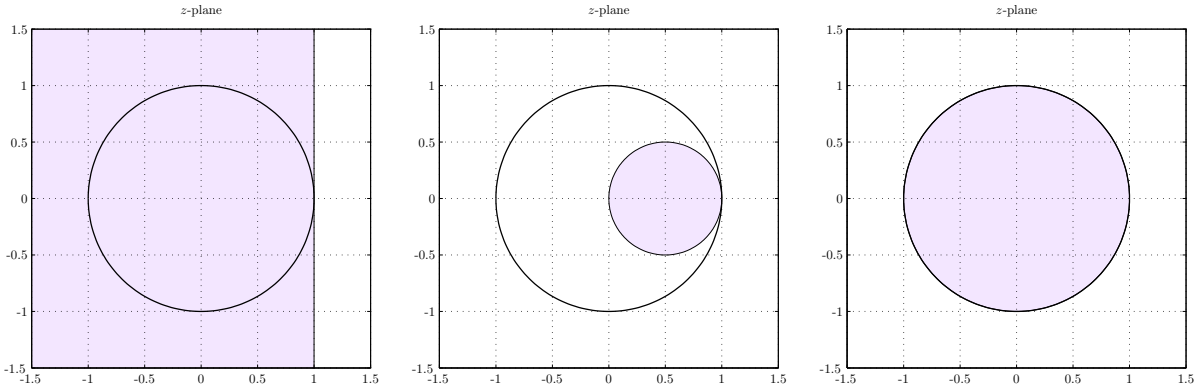

(a) Forward Euler method (b) Backward Euler method (c) Trapezoidal method

Figure 12: Mapping of the left–half s–plane onto the z–plane, with different discretization methods. The image of the left–half s–plane is highlighted with a shaded area.

in the z–plane, as shown in Fig. 12. From the figure, it can be immediately noticed that not all the methods of Tab. 1 guarantee that the discretization of a stable continuos–time controller is still stable: in particular, the forward Euler method may produce an unstable discrete–time controller even if the original continuous–time one is stable.

Note: the discretization procedure illustrated in (52) applies to a controller described in terms of its transfer function. If the controller is specified in terms of a state–space model, then alternative discretization formulas can be derived from (49), which directly relate the state–space matrices of the continuous–time model to those of the discrete–time counterpart. These formulas are summarised in Tab 3. For completeness, the discretization formulas for a controller specified in terms of its transfer function are reported in Tab. 2.

4.2 Direct digital design

The direct design in the discrete–time domain can be performed with any of the available classical or modern design methods, after having obtained a discrete–time model of the plant to be controlled with the *exact* discretization method illustrated in Sec. 3.2.

Forward Euler	Backward Euler	Trapezoidal	Exact
$C\left(\dfrac{z-1}{T}\right)$	$C\left(\dfrac{z-1}{T\,z}\right)$	$C\left(\dfrac{2}{T}\dfrac{z-1}{z+1}\right)$	$\left(1-z^{-1}\right)\mathcal{Z}\left\{\dfrac{C(s)}{s}\right\}$

Table 2: Discretization of a continuous–time transfer function $C(s)$.

	Forward Euler	Backward Euler	Trapezoidal	Exact
$\boldsymbol{\Phi}$	$\boldsymbol{I} + \boldsymbol{A}T$	$(\boldsymbol{I} - \boldsymbol{A}T)^{-1}$	$\left(\boldsymbol{I} + \frac{\boldsymbol{A}T}{2}\right)\left(\boldsymbol{I} - \frac{\boldsymbol{A}T}{2}\right)^{-1}$	$e^{\boldsymbol{A}T}$
$\boldsymbol{\Gamma}$	$\boldsymbol{B}T$	$(\boldsymbol{I} - \boldsymbol{A}T)^{-1}\boldsymbol{B}T$	$\left(\boldsymbol{I} - \frac{\boldsymbol{A}T}{2}\right)^{-1}\boldsymbol{B}\sqrt{T}$	$\int_0^T e^{\boldsymbol{A}\tau}\boldsymbol{B}\,d\tau$
$\boldsymbol{H}$	$\boldsymbol{C}$	$\boldsymbol{C}(\boldsymbol{I} - \boldsymbol{A}T)^{-1}$	$\sqrt{T}\boldsymbol{C}\left(\boldsymbol{I} - \frac{\boldsymbol{A}T}{2}\right)^{-1}$	$\boldsymbol{C}$
$\boldsymbol{J}$	$\boldsymbol{D}$	$\boldsymbol{D} + \boldsymbol{C}(\boldsymbol{I} - \boldsymbol{A}T)^{-1}\boldsymbol{B}T$	$\boldsymbol{D} + \boldsymbol{C}\left(\boldsymbol{I} - \frac{\boldsymbol{A}T}{2}\right)^{-1}\frac{\boldsymbol{B}T}{2}$	$\boldsymbol{D}$

Table 3: Discretization of a continuous–time state–space model $\Sigma_c = (\boldsymbol{A}, \boldsymbol{B}, \boldsymbol{C}, \boldsymbol{D})$.

5 Reduced–order state observers

An alternative to the use of a high–pass filter (i.e. "real derivative") for estimating the motor speed from the position measurement consists of using a *state observer*. The main advantage of using an observer is that the speed signal can be potentially determined without the phase lag error that invariably affects the estimate provided by any high–pass filter. A *reduced–order state observer* can be used for the estimation of the motor speed, since the other state variable, namely the motor position, is directly measured with a sensor (e.g. optical encoder). The general design procedure for a reduced–order state observer is summarised in the following Sec. 5.1 (continuous–time case) and Sec. 5.2 (discrete–time case).

5.1 Continuous–time design

The design procedure for a generic continuous–time reduced–order state observer is articulated in the following steps:

1. Let $\Sigma = (\boldsymbol{A}, \boldsymbol{B}, \boldsymbol{C}, \boldsymbol{0})$ be the state–space model of a continuous–time plant, whose state vector $\boldsymbol{x} \in \mathbb{R}^n$ has to be estimated. Assume that the model has m inputs and p outputs, and that $\operatorname{rank} \boldsymbol{C} = p$, i.e. all the plant outputs are linearly independent.

   Consider the state transformation $\boldsymbol{T}$ such that

   $$\boldsymbol{x}' = \boldsymbol{T}^{-1}\boldsymbol{x} = \begin{bmatrix}\boldsymbol{C}\\ \boldsymbol{V}\end{bmatrix} = \begin{bmatrix}\boldsymbol{y}\\ \boldsymbol{v}\end{bmatrix} \tag{53}$$

   where the $n - p$ rows of $\boldsymbol{V} \in \mathbb{R}^{(n-p)\times p}$ are chosen to be linearly independent with the p rows of $\boldsymbol{C}$. The vector $\boldsymbol{v} \in \mathbb{R}^{n-p}$ contains the unknown state variables to be estimated with the reduced–order state observer.

2. Rewrite the state model Σ in the new state variables $\boldsymbol{x}' = \boldsymbol{T}^{-1}\boldsymbol{x}$:

   $$\Sigma' : \begin{cases} \dot{\boldsymbol{y}} = \boldsymbol{A}'_{11}\,\boldsymbol{y} + \boldsymbol{A}'_{12}\,\boldsymbol{v} + \boldsymbol{B}'_1\,\boldsymbol{u} & (54)\\ \dot{\boldsymbol{v}} = \boldsymbol{A}'_{21}\,\boldsymbol{y} + \boldsymbol{A}'_{22}\,\boldsymbol{v} + \boldsymbol{B}'_2\,\boldsymbol{u} & (55)\end{cases}$$

3. Define the known input/output quantities:

$$\bar{\boldsymbol{u}} \triangleq \boldsymbol{A}'_{21}\,\boldsymbol{y} + \boldsymbol{B}'_2\,\boldsymbol{u} \tag{56}$$

$$\bar{\boldsymbol{y}} \triangleq \dot{\boldsymbol{y}} - \boldsymbol{A}'_{11}\,\boldsymbol{y} - \boldsymbol{B}'_1\,\boldsymbol{u} \tag{57}$$

so that the state–space model Σ' becomes:

$$\Sigma' : \begin{cases} \bar{\boldsymbol{y}} = \boldsymbol{A}'_{12}\,\boldsymbol{v} & (58) \\ \dot{\boldsymbol{v}} = \boldsymbol{A}'_{22}\,\boldsymbol{v} + \bar{\boldsymbol{u}} & (59) \end{cases}$$

which is a $(n-p)$-dimensional model with input $\bar{\boldsymbol{u}}$ and output $\bar{\boldsymbol{y}}$.

4. Design a full–order state observer for estimating the state vector $\boldsymbol{v} \in \mathbb{R}^{n-p}$ of Σ' , given the known input/output quantities $\bar{\boldsymbol{u}}$ and $\bar{\boldsymbol{y}}$. The equation of the state observer dynamics is

$$\begin{aligned} \dot{\hat{\boldsymbol{v}}} &= \boldsymbol{A}'_{22}\,\hat{\boldsymbol{v}} + \bar{\boldsymbol{u}} + \boldsymbol{L}\,(\bar{\boldsymbol{y}} - \boldsymbol{A}'_{12}\,\hat{\boldsymbol{v}}) \\ &= (\boldsymbol{A}'_{22} - \boldsymbol{L}\,\boldsymbol{A}'_{12})\,\hat{\boldsymbol{v}} + \underbrace{(\boldsymbol{A}'_{21}\,\boldsymbol{y} + \boldsymbol{B}'_2\,\boldsymbol{u})}_{\equiv\,\bar{\boldsymbol{u}}} + \boldsymbol{L}\,\underbrace{(\dot{\boldsymbol{y}} - \boldsymbol{A}'_{11}\,\boldsymbol{y} - \boldsymbol{B}'_1\,\boldsymbol{u})}_{\equiv\,\bar{\boldsymbol{y}}} \end{aligned} \tag{60}$$

5. To get rid of $\dot{\boldsymbol{y}}$ in (60) (the computation of the ideal derivative is practically unfeasible), introduce the new variable $\boldsymbol{z} \triangleq \hat{\boldsymbol{v}} - \boldsymbol{L}\,\boldsymbol{y}$. Then

$$\dot{\boldsymbol{z}} = \dot{\hat{\boldsymbol{v}}} - \boldsymbol{L}\,\dot{\boldsymbol{y}} = (\boldsymbol{A}'_{22} - \boldsymbol{L}\boldsymbol{A}'_{12})\,(\boldsymbol{z} + \boldsymbol{L}\boldsymbol{y}) + (\boldsymbol{A}'_{21}\,\boldsymbol{y} + \boldsymbol{B}'_2\,\boldsymbol{u}) + \boldsymbol{L}\,(-\boldsymbol{A}'_{11}\,\boldsymbol{y} - \boldsymbol{B}'_1\,\boldsymbol{u}) \tag{61}$$

After some computations, the equations of the reduced–order state observer become

$$\hat{\Sigma} : \begin{cases} \dot{\boldsymbol{z}} = \boldsymbol{A}_o\,\boldsymbol{z} + \boldsymbol{B}_o\,[\boldsymbol{u}\,,\,\boldsymbol{y}]^T & (62) \\ \hat{\boldsymbol{v}} = \boldsymbol{z} + \boldsymbol{L}\,\boldsymbol{y} & (63) \end{cases}$$

with

$$\begin{aligned} \boldsymbol{A}_o &= \boldsymbol{A}'_{22} - \boldsymbol{L}\,\boldsymbol{A}'_{12} \\ \boldsymbol{B}_o &= \left[\boldsymbol{B}'_2 - \boldsymbol{L}\,\boldsymbol{B}'_1\,,\quad (\boldsymbol{A}'_{22} - \boldsymbol{L}\,\boldsymbol{A}'_{12})\,\boldsymbol{L} + \boldsymbol{A}'_{21} - \boldsymbol{L}\,\boldsymbol{A}'_{11}\right] \end{aligned} \tag{64}$$

6. The estimate of the original state vector is given by

$$\hat{\boldsymbol{x}} = \boldsymbol{T}\,\hat{\boldsymbol{x}}' = \boldsymbol{T}\begin{bmatrix}\boldsymbol{y} \\ \hat{\boldsymbol{v}}\end{bmatrix} \tag{65}$$

Therefore, the equations of the reduced–order state observer in the original state variables are

$$\hat{\Sigma} : \begin{cases} \dot{\boldsymbol{z}} = \boldsymbol{A}_o\,\boldsymbol{z} + \boldsymbol{B}_o\,[\boldsymbol{u},\,\boldsymbol{y}]^T & (66) \\ \hat{\boldsymbol{x}} = \boldsymbol{C}_o\,\boldsymbol{z} + \boldsymbol{D}_o\,[\boldsymbol{u},\,\boldsymbol{y}]^T & (67) \end{cases}$$

with

$$\boldsymbol{C}_o = \boldsymbol{T}\begin{bmatrix}\boldsymbol{0}_{p\times(n-p)} \\ \boldsymbol{I}_{(n-p)\times(n-p)}\end{bmatrix}, \qquad \boldsymbol{D}_o = \boldsymbol{T}\begin{bmatrix}\boldsymbol{0}_{p\times m} & \boldsymbol{I}_{p\times p} \\ \boldsymbol{0}_{(n-p)\times m} & \boldsymbol{L}\end{bmatrix} \tag{68}$$

The design of the reduced–order state observer consists of finding the gain matrix $\boldsymbol{L} \in \mathbb{R}^{(n-p)\times p}$ such that the eigenvalues of $\boldsymbol{A}_o = \boldsymbol{A}'_{22} - \boldsymbol{L}\,\boldsymbol{A}'_{12}$ are placed at certain desired locations in the open left–half complex plane. This corresponds to assign a prescribed rate of convergence of the estimation error $\tilde{\boldsymbol{v}} = \boldsymbol{v} - \hat{\boldsymbol{v}}$ to zero, since this quantity is governed by the dynamical equation $\dot{\tilde{\boldsymbol{v}}} = \boldsymbol{A}_o\,\tilde{\boldsymbol{v}}$. The arbitrary placement of the observer eigenvalues is possible if and only if the pair $(\boldsymbol{A}'_{22},\, \boldsymbol{A}'_{12})$ is observable. It can be proved that a sufficient condition for the observability of the pair $(\boldsymbol{A}'_{22},\, \boldsymbol{A}'_{12})$ is that the pair $(\boldsymbol{A}',\, \boldsymbol{C}')$ is observable or, alternatively, that the pair $(\boldsymbol{A},\, \boldsymbol{C})$ is observable, since observability is invariant for linear state transformations.

5.2 Discrete–time design

The design procedure for a discrete–time reduced–order observer is virtually identical to that of the continuous–time counterpart. Let $\Sigma = (\boldsymbol{\Phi},\, \boldsymbol{\Gamma},\, \boldsymbol{H},\, \boldsymbol{J})$ be the state–space model of a discrete–time plant, whose state vector $\boldsymbol{x} \in \mathbb{R}^n$ has to be estimated. By following the procedure illustrated in Sec. 5.1 (with obvious adaptations for dealing with the discrete–time case), it can be easily verified that the discrete–time reduced–order state observer is described by the following equations:

$$\hat{\Sigma}\ :\ \begin{cases} \boldsymbol{z}[k+1] \;=\; \boldsymbol{\Phi}_o\,\boldsymbol{z}[k] \;+\; \boldsymbol{\Gamma}_o\,[\boldsymbol{u}[k],\ \boldsymbol{y}[k]]^T & (69) \\ \hat{\boldsymbol{x}}[k] \;=\; \boldsymbol{H}_o\,\boldsymbol{z}[k] \;+\; \boldsymbol{J}_o\,[\boldsymbol{u}[k],\ \boldsymbol{y}[k]]^T & (70) \end{cases}$$

with

$$\begin{aligned} \boldsymbol{\Phi}_o \;&=\; \boldsymbol{\Phi}'_{22} - \boldsymbol{L}\,\boldsymbol{\Phi}'_{12} \\ \boldsymbol{\Gamma}_o \;&=\; \left[\boldsymbol{\Gamma}'_2 - \boldsymbol{L}\,\boldsymbol{\Gamma}'_1\,,\quad (\boldsymbol{\Phi}'_{22} - \boldsymbol{L}\,\boldsymbol{\Phi}'_{12})\,\boldsymbol{L} + \boldsymbol{\Phi}'_{21} - \boldsymbol{L}\,\boldsymbol{\Phi}'_{11}\right] \end{aligned} \tag{71}$$

and

$$\boldsymbol{H}_o \;=\; \boldsymbol{T}\begin{bmatrix} \boldsymbol{0}_{p\times(n-p)} \\ \boldsymbol{I}_{(n-p)\times(n-p)} \end{bmatrix}, \qquad \boldsymbol{J}_o \;=\; \boldsymbol{T}\begin{bmatrix} \boldsymbol{0}_{p\times m} & \boldsymbol{I}_{p\times p} \\ \boldsymbol{0}_{(n-p)\times m} & \boldsymbol{L} \end{bmatrix} \tag{72}$$

where $\boldsymbol{T}$ is the state transformation that partitions the state vector $\boldsymbol{x}$ as specified in (53), and

$$\boldsymbol{\Phi}' \;=\; \boldsymbol{T}^{-1}\,\boldsymbol{\Phi}\,\boldsymbol{T} \;=\; \begin{bmatrix} \boldsymbol{\Phi}'_{11} & \boldsymbol{\Phi}'_{11} \\ \boldsymbol{\Phi}'_{21} & \boldsymbol{\Phi}'_{22} \end{bmatrix}, \qquad \boldsymbol{\Gamma}' \;=\; \boldsymbol{T}^{-1}\,\boldsymbol{\Gamma} \;=\; \begin{bmatrix} \boldsymbol{\Gamma}'_1 \\ \boldsymbol{\Gamma}'_2 \end{bmatrix} \tag{73}$$